Imperial Journal of Interdisciplinary Research (IJIR)
Vol-3, Issue-2, 2017
ISSN: 2454-1362, http://www.onlinejournal.in

Structural Analysis of Nano Titanium Dioxide in Phase Transition Region

Sanjeev Kumar
Department of Physics, Rajiv Gandhi University, Itanagar
Arunachal Pradesh ,India-791112

Abstract: *Nanostructured Titanium dioxide (TiO_2) powder has been prepared by sol-gel method sintered at different thermal treatments during same period of time. Nano powders contained brookite, anatase, rutile and/or the coexistence of all of them. Phase transition has been observed as amorphous to anatase phase and anatase to the rutile phase gradually in TiO_2 as the sintering temperature increased. The effect of zinc dopant on the phase transition of TiO_2 at different calcine temperature has been studied. In this work, X-ray diffraction of nanocrystalline TiO2 has been undertaken to obtain structural data (lattice parameters, tetragonality, and position coordinates) and microstructural data during the meta stable to stable transformation. Change in isoelectric point (IEP) during meta stable-to-stable transformation in TiO_2 has been also studied by zeta potential. The average crystallite size increased from 10 nm to 100 nm. A band edge shift of 0.2eV has been observed in the $(\alpha h\upsilon)^2$ versus $h\upsilon$ plot.*

Introduction

Among various oxide semiconductor photocatalysts, Titanium dioxide (TiO_2) is the most important photocatalyst because of its biological and chemical inertness, nontoxicity, cost effectiveness and strong oxidizing power under UV light irradiation [1-5]. Titanium dioxide is a naturally occurring oxide of titanium and has been studied extensively due to the wide range of its applications and the expectation for insights into surface and structural properties on the fundamental level. It is a good photocatalyst with relatively high efficiency for the decomposition of water and organic molecules [6-11]. The density of surface defect sites of the TiO_2 generally responsible for the photocatalytic propetiy. Liu et al. have shown that the dominant defects in TiO_2 surfaces are Ti^{3+} defects and oxygen vacancies [12]. Moreover, this material would have new industrial applications including antibacterial ceramic tiles, self-cleaning glass and so on [13]. Hydrogen treated TiO2 gains a dramatic increase in conductivity making large bandgap semiconductor a promising current collector [14]. However, this study involved only the structural change during sythesis, primary particle size, and crystal phase. It has been reported that these properties of TiO_2 nanoparticle can affect its photocatalytic activity [15] and toxicity [16].

Anatase is generally considered the most efficient TiO_2 polymorph in photocatalytic reactions, whereas the activity of the rutile phase can be strongly affected by the preparation conditions [17] Only few studies examined the photocatalytic behaviour of brookite so far[18-20]. Recently, brookite has been used the photocatalytic production of hydrogen [21,22]. Generally, anatase/brookite mixtures and pure brookite were found to be more photoactive than pure anatase or rutile. Thus, the photocatalytic performance of brookite deserves a more in depth investigation.

In the present work the effect of the crystal structure of TiO_2 has been systematically investigated in relation to it's the calcine temperature and doping Zn- ions. It has been investigated together band gap energies and isoelectric point (IEP) with a series of samples with different doping concentration .

Experiment details

We did ultrasonic cleaning after washed all vessels and glasswares with detergent. To synthesize Titanium dioxide we have taken 40 ml of 2-proanol and 20 ml of titanium tetra iso-propoxide ($C_{12}H_{28}O_4Ti$) in a beaker stair well around approximately 15min to make (Solution-1). Now take another beaker in 25 ml of 2-propanol and zinc nitrate hexa hydrate($Zn(No_3)_2.6H_2o$) stair well around 15min (Solution-2). Then we have mixed the solution-2 in solution-1 drop wise and stair well around 30min. Then start the drop wise addition of the ammonia in main beaker and maintain the PH around 8 to 9. Before start filtration, wash the sample by help the 2-propanol .then start filtration by the help of the filter paper. Take the filtrate zinc doped Tio2in dish and put in oven at temperature 80°c and made the amorphous zinc doped Tio_2. Then we started heating the product in furnace for calcinations at different temperature for 2 hours. We found the desired material of TiO_2. The obtained materials has been characterized by X-ray diffraction for structural

analysis, zeta potential to see Isoelectric point (IEP). To find the band gap we perform the absorption spectroscopy. Scanning electron microscopy has been used to see the morphology of the synthesized titanium dioxide.

Result and discussion

One of the aspects for efficiency using nana structured TiO2 for these applications is to understand the science behind the tailor-making nanostructures with respect to crystal structure, phase, crystal size. Meta stable-to-stable transformation in oxide are interesting for both scientific and technology concern due to the drastically changes in these surface properties. TiO2 exists in three crystalline phase namely, anatase (tetragonal, space group: $I4_1/amd$, and density~ 3.9g/cc), rutile (tetragonal, space group: $P4_2$),Brookite (space group: Pbca). Figure:1 (A) shows X-ray diffraction pattern of pure TiO2 calcination at different temperature, at start calcination temperature 300^{O}C,the sample remain in amorphous phase and increase the calcination temperature 350 ^{O}C to 600 ^{O}C and the amorphous phase is transfer to the Anatase phase at 400 ^{O}C, then after increase the calcination temperature Anatase phase is transfer to the Rutile phase. How the rutile phase is going to dominant over anatase with the calcine temperature has been shown in figure 1 (B).

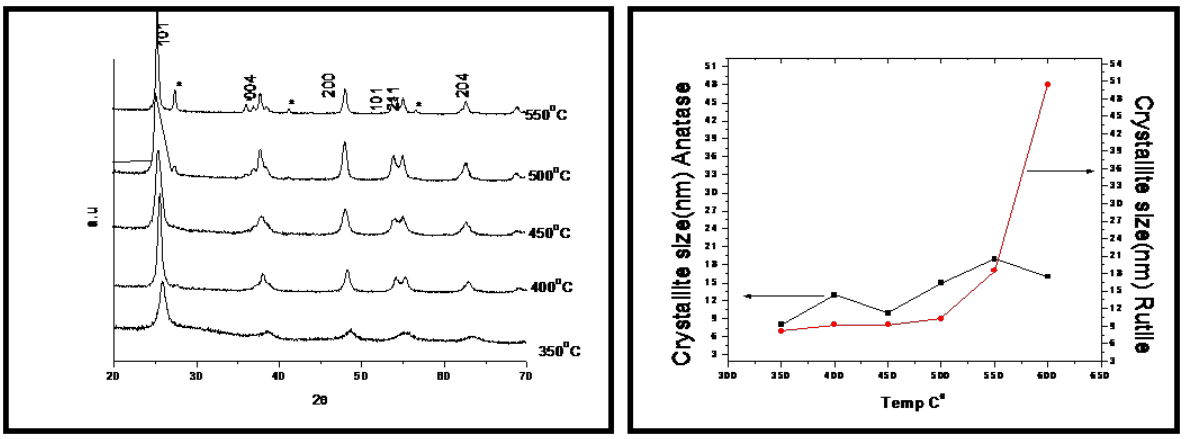

A **B**

Figure 1(A)X-ray diffraction pattern of pure TiO2 at different calcine temperatures * shows the rutile phase (B) Crystallite size V/S Temperature (Pure TiO_2)

Anatase and brookite are metastable phases, whereas rutile is the most stable phase. Brookite and anatase convert to rutile when they are calcined at higher temperatures. The phase transition temperature varies with the method of preparation of the powders. All of these phases consist of TiO_6^{2-}octahedra as shown in figure 2. For the formation of titanium dioxide crystal, first two octahedron condense together to form a bond as shown in figure. Then position of the third octahedral determines the phase that will be formed. Rutile has a tetragonal structure, theoctahedron join in such a way that they form a linear chain and so just two of the twelve edges of the octahedra are connected. The linear chain is joined by sharing of corner oxygen atoms. Figure 2 (B) shows the transformation mechanism of anatase phase to rutile phase by joining of two edges of the octahedral. Anatase also has a tetragonal structure. In anatage there is no corner oxygen sharing.

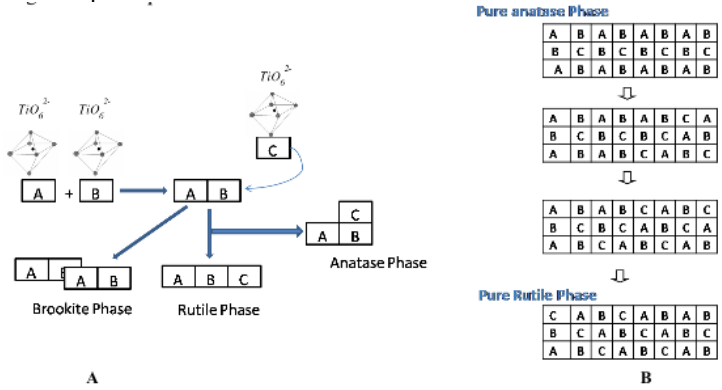

Figure 2(A) Formation mechanism of three phase of TiO_2 (B) Transformation mechanism of Anatase to rutile Phase.

Doping on metal –ions in TiO_2 always challenge for researchers due mismatch of lattice parameter. The ionic radii of Zn^{2+} (0.74 Å) is similar to that of host Ti^{4+} (0.75 Å) ions. Hence this ion can easily substitute Ti^{4+} ion in TiO2 lattice without distorting the crystal structure, thereby stabilizing the anatase phase over a range of dopant concentrations. We have studied the effect of zinc dopant on the phase transision at different calcine temperature. Figure:3 shows the XRD pattern of doped TiO2 at different level of concentration of dopant at different calcine temperature. The sample was perfectly in anatase phase at all level of dopant. We could not observe any other spinel of zinc and titanium. We can attribute the access amount of zinc ion can make compound but it was in amorphous phase. So, at 400°C temperature it is difficult to see any other phase beside the anatase. While a change in the lattice parameter could be due the doping at atomic level of TiO2 as shown. It is interesting to note that the values of 'a' and 'c' first decrease as Zn is increased up to 2 mole percent then increases. According to Vegard'slaw change in lattice parameter with doping percentage should vary linearly, however, it is not the case in present study.

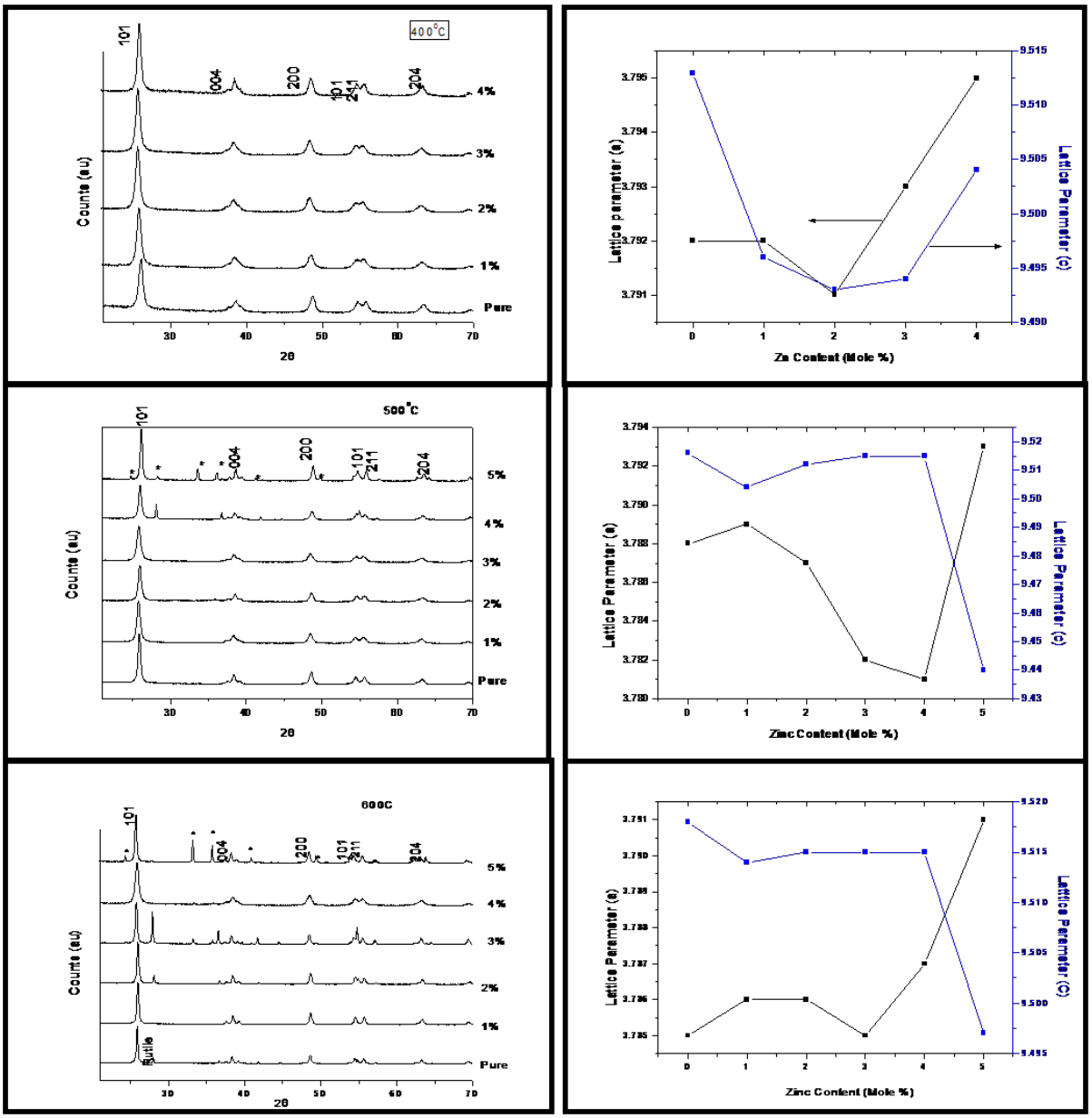

A **B**

Figure3(A)X-ray diffraction pattern of zinc doped TiO_2 at diffrent temperature (B)zinc content V/S lattice parameter

The deviations from the linearity or from Vegard's law can be attributed to the interstitial incorporation of Zn in TiO_2 and to the fact that at higher concentration Zn is not soluble into TiO_2. It has been observed there are seven XRD peaks up to 3 mole percent of zinc, and all these peaks are indexed as anatase TiO_2,however, for all more concentrations more peaks start appearing in addition to these seven peaks. One may note that as Zn-doping is increased to 5 Mole % some additional peaks start emerging and become more prominent at higher concentration. There additional peaks (*) were index as the Zinc Titanium Oxide ($ZnTiO_3$ ICCD 85-0547). It has been also observe a change in lattice parameter of zinc doped titainia at 500^OC. It is interested to observe lattice parameter 'a' is decreased and lattice parameter 'c' is linear up 4 mole % concentration of Zinc. As increase the concentration more than 4 mole % lattice parameter 'a' drastically increase and 'c' drastically decrease. It could be the approach to deform of the crystal structure of TiO_2 on high concentration of zinc toward the rutile phase.

It has been observed from Figure :4.8that there are seven XRD peaks up to 4 mole percent of zinc, and all these peaks are indexed asanatase TiO_2,however, for all more concentrations more peaks start appearing in addition to these seven peaks. One may note that as Zn-doping is increased to 5 Mole % some additional peaks start emerging and become more prominent at higher concentration. There additional peaks (*) were index as the Zinc Titanium Oxide ($ZnTiO_3$ ICCD 85-0547).

We observe a change in lattice parameter of zinc doped titainia at 600^OC. It is interested to observe lattice parameter 'a' is decreased and lattice parameter 'c' is linearup 3 mole % concentration of Zinc. As increase the concentration more than 4 mole % lattice parameter 'a' drastically increase and 'c' drastically decrease. It could be the approach to deform of the crystal structure of TiO_2 on high concentration of zinc toward the rutile phase.

Figure:4 shows at increase the calcination temperature, linearly increase the zeta potential of the Zn doped TiO_2 and the particle size will be decrease. So the effective surface charge on the particle depends on the isoelectric point (IEP) in the suspension. The PH value of the dispersion medium of a colloidal suspension at which the colloidal particles do not move in the electric field is called isoelectric point (IEP). 5mole% of Zn doped TiO_2 will be high surface charge compare to other .so it indicate that the batter stability of these particles. Figure shows Pure TiO_2calcination at different temperature, so linearly increase the zeta potential. Effective surface charge on the particle depends up on the isoelectric point(IEP) and the at the calcination temperature 600°c pure TiO_2 high surface charge compare to other and also indicate the that batter stability of these particles.

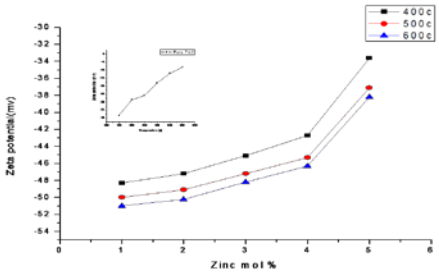

Figure 4. Zeta potential of Zinc doped Tio$_2$

The dependence of Absorption coefficient on energy (hυ) near the band edge for Zn-doped TiO_2nana particles is shown in Fig.5 .In a crystalline or polycrystalline material, direct or indirect optical transitions are possible depending on the band structure of the material. It was suggested that the extended absorption-edge spectrum of a normal direct band gap semiconductor, such as TiO_2. The usual method of determining band gap is to plot a graph between αhυ and hυ according Tauc Relation.

$$\alpha h\nu = A(h\nu - E_g)^n$$

where hυ is the photon energy, α is the absorption coefficient, Eg is the energy band gap, A is the constant and n is 1/2 for the direct band gap. A band edge shift of 0.2eV has been estimated form the $(\alpha h\upsilon)^2$ versus hυ plot.

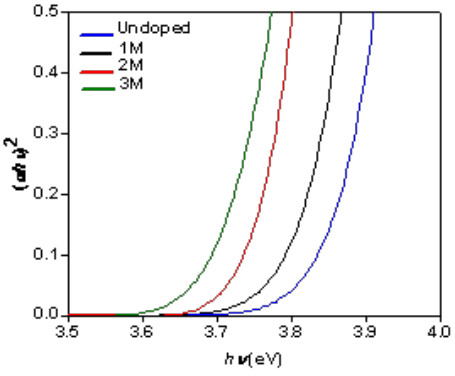

Figure5: Band gap calculation of Zn doped TiO_2

Conclusion:

In TiO2 the rutile phase is going to dominant over anatase with increase the

calcination temperature 350 ^{O}C to 600 ^{O}C. The amorphous phase is transfer to the Anatase phase at 400 ^{O}C, then after increase the calcination temperature Anatase phase is transfer to the Rutile phase. At 4 mole% of zinc as dopant, shows the asanatase TiO_2 while Zn-doping is increased to 5 Mole % some additional peaks start emerging and become more prominent at higher concentration. It could be the approach to deform of the crystal structure of TiO_2 on high concentration of zinc toward the rutile phase. Effective surface charge on the particle depends up on the isoelectric point(IEP) and the at the calcination temperature 600°c pure TiO_2 high surface charge compare to other and also indicate the that batter stability of these particles. There is not much effect of zinc doping on the band gap while zinc doping disturbing the phase stability of TiO_2.

Acknowledgement:

Author would like to acknowledge Prof D O Shah and Mr Harshal Pandya, for their kind support and help during data acquisition at Shah Schulman Center for Surface Science and Nanotechnology Nadiad Gujarat.

References:

1. Cui Lai, Man-Man Wang, Guang-Ming Zeng, Yun-Guo Liu, Dan-Lian Huang, Cheng Zhang, Rong-Zhong Wang, Piao Xu, Min Cheng, Chao Huang, Hai-Peng Wu, Lei Qin, *Applied Surface Science* **390** (2016), 368.
2. Chunlin Lu, Lin Zhang, Yunwang Zhang, Shenye Liu, *Materials Letters* **185** (2016), 342.
3. Xiaopeng Wang, Shouqiang Huang, Nanwen Zhu, Ziyang Lou, Haiping Yuan, *Applied Surface Science* **359** (2015), 917.
4. Li-Fen Chiang and Ruey-an Doong, *Separation and Purification Technology* **156** (2015), 1003.
5. Yeongsoo Choi, T. Umebayashi and M. Yoshikawa, *Journal of Material Science* **39** (2004), 1837.
6. Fujishima and K. Honda, *Nature* **238** (1972), 37.
7. A. J. Nozik, *Nature* **257** (1975), 383.
8. J. H. Carey and B. G. Oliver, *Nature* **259** (1976), 554.
9. J. Tang, J. R. Durrant and D. R. Klug, *Journal of the American Chemical Society* **130** (2008), 13885.
10. S. Liu, J. Yu and M. Jaroniec, *Journal of the American Chemical Society* **132** (2010), 11914.
11. K. Lee, D. Kim and P. Roy I. Paramasivam, B. I. Birajdar, E. Spiecker and P. Schmuki, *Journal of the American Chemical Society* **132** (2010), 1478.
12. H. Liu, H. T. Ma, X. Z. Li, W. Z. Li, M. Wu and X. H. Bao, *Chemosphere* **50** (2003), 39.
13. C. Sciancalepore, T. Manfredini and F. Bondioli, *Advances in Science and Technology* **92** (2014), 90.
14. Zheng Liang, Guangyuan Zheng, Weiyang Li, Zhi Wei Seh, Hongbin Yao, Kai Yan and Desheng Kong, *Nano* **8** (2014), 5249.
15. CB Almquist and P. Biswas, *J Catal* **212** (2002), 145.
16. LK Braydich-Stolle, NM Schaeublin, RC Murdock, J Jiang, P Biswas, JJ Schlager, SM Hussain, *J Nanopart Res* **11** (2009), 1361.
17. A. Sclafani, L. Palmisano and M. Schiavello, *J. Phys. Chem* **94** (1990), 829.
18. A. Di Paola, M. Addamo, M. Bellardita, E. Cazzanelli and L. Palmisano, *Thin Solid Films* **515** (2007), 3527.
19. M. Addamo, M. Bellardita, A. Di Paola and L. Palmisano, *Chem. Commun.* (2006), 4943.
20. M. Addamo, V. Augugliaro, M. Bellardita, A. Di Paola, V. Loddo, G. Palmisano, L. Palmisano and S. Yurdakal, *Catal. Lett.* **126** (2008), 58.
21. T. A.Kandiel, A. Feldhoff, L. Robben, R. Dillert and D. W. Bahnemann, *Chem. Mater* **22** (2010), 2050.
22. B. I. Lee, S. Kaewgun, W. Kim, W. Choi, J. S. Lee and E. Kim, *j. Renewable Sustainable Energy* **1** (2009), 023101.